Dyes and Pigments 82 (2009) 58–64

Contents lists available at ScienceDirect

Dyes and Pigments

journal homepage: www.elsevier.com/locate/dyepig

The design of a novel fluorescent PET sensor for proton and water: A phenylaminonaphtho[1,2-*d*]oxazol-2-yl-type fluorophore containing proton donor and acceptor groups

Yousuke Ooyama [a,*], Haruka Egawa [b], Katsuhira Yoshida [a,b,**]

[a] Department of Material Science, Faculty of Science, Kochi University, Akebono-cho, Kochi 780-8520, Japan
[b] JST (Japan Science and Technology Agency) Satellite Kochi 2-17-47, Asakurahommachi, Kochi 780-8073, Japan

ARTICLE INFO

Article history:
Received 8 September 2008
Received in revised form
4 November 2008
Accepted 4 November 2008
Available online 24 November 2008

Keywords:
Photo-induced electron transfer
Fluorescence
Zwitter-ion form
Fluorescent PET sensor
Water

ABSTRACT

Novel phenylaminonaphtho[1,2-*d*]oxazol-2-yl-type fluorophores having a diethylamino group as proton binding site and a carboxyl group as proton donating site, for sensing protons and water, have been designed and developed, and their photophysical properties were investigated in solution. In 1,4-dioxane, fluorophores that did not contain a proton binding site exhibited an intense fluorescence band whereas fluorophores that contained a proton binding site displayed only a weak fluorescence band. However, this behavior was reversed when the two types of fluorophore were dissolved in aq. acetic acid solution. The fluorophore that contained both a proton binding site and proton donating site showed weak fluorescence in organic solvents, but very intense fluorescence accompanied an increase in the water content of such solvents. Semi-empirical molecular orbital calculations (AM1 and CNDO/S) and spectral analyses revealed that such fluorophores are capable of sensing protons or water by photo-induced electron transfer.

1. Introduction

The design and development of fluorescent sensors are of major importance because their possible applications as optical, biochemical, and medical sensors as well as optoelectronic devices [1–6]. Fluorescent, photo-induced electron transfer (PET) sensors are especially useful for the detection of cations such as Na^+, K^+, Ca^{2+}, Mg^{2+}, Cu^{2+}, Zn^{2+}, Pb^{2+}, and Cd^{2+} including protons (H^+) [7–22]. Almost all fluorescent PET sensors are composed of a fluorophore skeleton linked to a cation binding site such as an amino moiety via a methylene spacer. For example, there are some PET sensors which are composed of anthracene as the fluorophore skeleton and an mono-azacrown ether as cation binding site [1–5,15]. In this case, photo-induced electron transfer occurs from the nitrogen atom of mono-azacrown ether to anthracene and results in fluorescence quenching of the fluorophore. When the nitrogen atom is either protonated or when it strongly interacts with a cation, this electron transfer mechanism is prevented and a drastic enhancement of fluorescence is observed. The fluorescent dye for sensing water in an organic solvent is also of interest in fundamental research on analytical chemistry and is also important for industrial applications [23–26]. Some fluorescent water sensors have been developed, which exhibit changes of their fluorescence lifetime and intensity with varying amounts of water content in organic solvents [27,28]. However, in almost all cases, the fluorescence intensity decreases with increasing water content [29–34], which can be attributed to both a specific water-fluorophore interaction as well as an increase in the polarity of the solvent mixture. Hence, the exact determination of water content in a solution is difficult using such fluorescent dyes, as the fluorescence intensity is strongly affected by the polarity of the solution.

In previous work, the present authors reported a new class of fluorescent dye for sensing water in organic solvents based on the phenylaminonaphtho[1,2-*d*]oxazol-2-yl-type fluorophore **1d** that contains both a proton binding site and proton donating site; the fluorophore exhibited weak fluorescence in organic solvents, but a drastic enhancement of fluorescence intensity was observed with an increase in the water content of the organic solvent. However, such absorption and fluorescence properties were not observed in the cases of **1a**, **1b**, **1c**, and **1e** (Scheme 1) [35]. Furthermore, we recently found that the fluorophores **1c**–**1e** exhibit an enhancement in the fluorescence intensity with an increase of acid content in organic solvents. In this paper, we report the mechanism of the fluorescent sensor system for detecting proton and water based on phenylaminonaphtho[1,2-*d*]oxazol-2-yl-type fluorophores. In order to elucidate the effects of the proton binding and proton

* Corresponding author. Fax: +81 88 844 8359.
** Corresponding author. Department of Material Science, Faculty of Science, Kochi University, Akebono-cho, Kochi 780-8520, Japan.
E-mail addresses: yooyama@hiroshima-u.ac.jp (Y. Ooyama), kyoshida@cc.kochi-u.ac.jp (K. Yoshida).

0143-7208/$ – see front matter © 2008 Elsevier Ltd. All rights reserved.
doi:10.1016/j.dyepig.2008.11.002

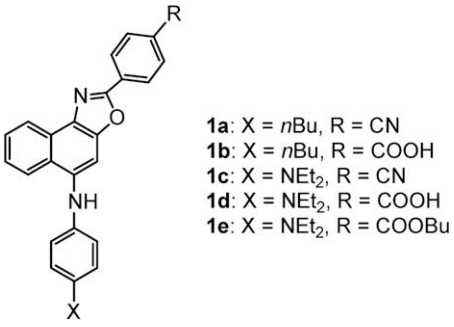

Scheme 1. Chemical structures of the fluorophores **1a**–**1e**.

donating groups and the fluorophore skeleton on photophysical properties of the fluorophores, it was decided to elucidate the photophysical properties of the dyes in various solutions and to undertake semi-empirical molecular orbital calculations (AM1 and CNDO/S). On the bases of these calculations and spectral analyses, it was observed that the phenylaminonaphtho[1,2-*d*]oxazol-2-yl-type fluorophores **1c**–**1e** constitute a class of fluorescent dyes that can be used for sensing both protons and water by photo-induced electron transfer.

2. Experimental

Absorption spectra were observed with a JASCO U-best30 spectrophotometer. For the measurement of the emission spectra, a JASCO FP-777 spectrometer was used. The fluorescence quantum yields (Φ) in organic solvents were determined using 9,10-diphenylanthracene (Φ = 0.67, λ_{ex} = 357 nm) in benzene as the standard. The Φ values in a mixture solvent of organic solvent and water or acetic acid were determined by using a calibrated integrating sphere system (λ_{ex} = 325 nm).

2.1. Computational methods

All calculations were performed on FUJITSU FMV-ME4/657. The semi-empirical calculations were carried out with the WinMOPAC Ver. 3 package (Fujitsu, Chiba, Japan). Geometry calculations in the ground state were carried out using the AM1 method [36]. All geometries were completely optimized (keyword PRECISE) by the eigenvector following routine (keyword EF). Experimental absorption spectra of the seven quinol derivatives were studied with the semi-empirical method CNDO/S (intermediate neglect of differential overlap/spectroscopic) [37–40]. All CNDO/S calculations were performed using single excitation full SCF/CI (self-consistent field/configuration interaction), which includes the configuration with one electron excited from any of the highest 25 occupied orbital to any of the lowest 25 unoccupied orbital, 225 configurations were considered for the configuration interaction [keyword CI (15 15)].

3. Results and discussion

3.1. Spectroscopic properties of phenylaminonaphtho[1,2-d]oxazol-2-yl-type fluorophores in solution

The fluorophores **1a** and **1b** exhibit a weak absorption band at around 335 nm and an intense absorption band at around 400 nm, and a single intense fluorescence band at around 495 nm (Φ = 0.92–0.95) in 1,4-dioxane (Fig. 1). The absorption maxima of **1a** and **1b** were affected slightly by changing the solvent from 1,4-dioxane to acetone, while the fluorescence maxima show a large bathochromic shift. Therefore, the Stokes shift value in polar solvents became greater than that in non-polar solvents. Significant

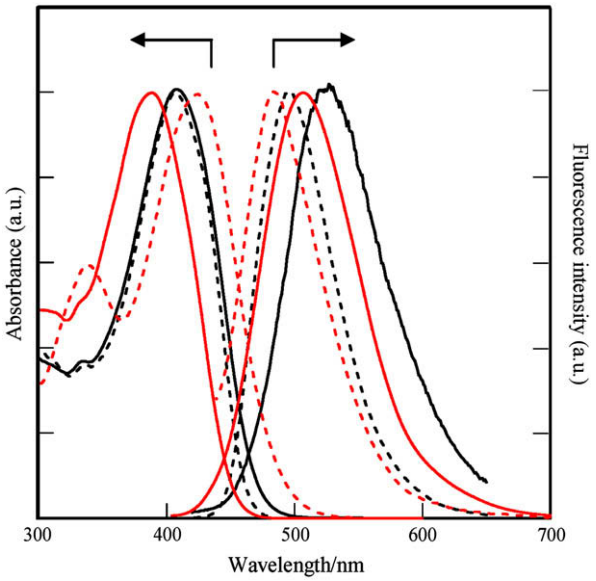

Fig. 1. Absorption and fluorescence spectra of **1a** (black) and **1c** (red) in 1,4-dioxane (dotted line) and acetic acid (solid line).

dependence of the fluorescence quantum yield on the solvent polarity was also observed: the Φ value of **1a** is reduced to *ca.* 4% with increasing polarity from 1,4-dioxane to acetone. Similar spectral changes are generally observed for most of fluorescent dyes whose dipole moments in the excited state are larger than those in the ground state [41,42].

In contrast, the fluorophores **1c**–**1e** exhibited two absorption bands at around 420 nm and 350 nm, and a weak fluorescence band at around 490 nm in 1,4-dioxane (Fig. 1). As with the fluorophores **1a** and **1b,** the dependence of the fluorescence maxima on the solvent polarity was observed; however, its dependence was smaller for **1d** and **1e**. With increasing polarity of the solvent, the Φ value of **1c**, **1d**, and **1e** was also reduced. Interestingly, in acetic acid, the fluorophores **1c**–**1e** exhibited a medium fluorescence intensity (Φ = 0.18–0.20); however, the fluorophores **1a** and **1b** exhibited

Table 1
Spectroscopic properties of **1a**–**1e** in solution

	Solvent	λ^{abs}_{max}/nm[a] [ε_{max}/dm^3 mol^{-1} cm^{-1}]	λ^{fl}_{max}/nm[b]	Φ[c]
1a	benzene	406 (24,300), 335 (9000)	477	0.86
	1,4-dioxane	407 (24,200), 335 (8700)	495	0.92
	dichloromethane	408 (25,400), 336 (8500)	517	0.83
	acetone	410 (26,900), 335 (9200)	545	0.04
	ethanol	416 (24,000), 334 (8500)	542	0.03
	acetic acid	408 (25,200), 334 (9200)	524	0.04
1b	1,4-dioxane	400 (20,700), 336 (8600)	491	0.95
	acetone	401 (26,100), 332 (9900)	534	0.66
	acetic acid	406 (25,000), 335 (9800)	535	0.03
1c	benzene	420 (31,700), 350 (18,600)	485	1.0×10^{-3}
	1,4-dioxane	420 (25,300), 350 (15,500)	483	1.0×10^{-3}
	dichloromethane	420 (23,700), 349 (14,200)	498	2.0×10^{-3}
	acetone	420 (24,200), 350 (15,000)	527	1.0×10^{-3}
	ethanol	431 (25,300), 350 (15,300)	538	1.0×10^{-3}
	acetic acid	387 (23,300), 311 (11,300)	504	0.18
1d	1,4-dioxane	413 (23,800), 338 (15,400)	490	1.0×10^{-3}
	acetone	413 (21,100), 338 (13,600)	508	3.0×10^{-4}
	ethanol	400 (20,700), 328 (13,400)	493	6.0×10^{-5}
	acetic acid	385 (24,500), 312 (12,800)	520	0.2
1e	1,4-dioxane	415 (25,800), 337 (15,800)	500	2.0×10^{-3}
	acetone	417 (26,000), 339 (16,100)	526	4.0×10^{-5}
	acetic acid	384 (24,000), 312 (10,000)	509	0.2

[a] 2.5×10^{-5} M.
[b] 2.5×10^{-6} M.
[c] The Φ value were determined using 9,10-diphenylanthracene (Φ = 0.67, λ_{ex} = 357 nm) in benzene as the standard.

Table 2
Spectroscopic properties of **1a**–**1e** in acidic solution

	Solvent	λ_{max}^{abs}/nm[a]	λ_{max}^{fl}/nm[b]	Φ[c]
		[ε_{max}/dm^3 mol^{-1} cm^{-1}]		
1a	1,4-dioxane-acetic acid (5 vol%)	408 (27,600), 335 (9900)	499	0.91
	1,4-dioxane-acetic acid (20 vol%)	409 (25,000), 334 (8500)	510	0.51
	1,4-dioxane-acetic acid (40 vol%)	409 (24,300), 333 (8500)	520	0.23
	acetic acid	408 (25,200), 334 (9200)	524	0.04
1b	1,4-dioxane-acetic acid (5 vol%)	402 (27,700), 333 (10,800)	505	0.92
	1,4-dioxane-acetic acid (20 vol%)	403 (26,100), 333 (9900)	522	0.52
	1,4-dioxane-acetic acid (40 vol%)	404 (25,400), 332 (10,000)	534	0.17
	acetic acid	406 (25,000), 335 (9800)	535	0.03
1c	1,4-dioxane-acetic acid (5 vol%)	424 (22,100), 340 (13,800)	482	0.03
	1,4-dioxane-acetic acid (20 vol%)	416 (21,400), 340 (13,500)	489	0.07
	1,4-dioxane-acetic acid (40 vol%)	394 (23,200), 337 (12,000)	497	0.16
	acetic acid	387 (23,300), 311 (11,300)	504	0.18
1d	1,4-dioxane-acetic acid (5 vol%)	413 (24,500), 339 (15,900)	494	0.02
	1,4-dioxane-acetic acid (20 vol%)	403 (20,700), 339 (13,800)	498	0.06
	1,4-dioxane-acetic acid (40 vol%)	389 (24,700), 334 (14,100)	510	0.15
	acetic acid	385 (24,500), 312 (12,800)	520	0.2
1e	1,4-dioxane-acetic acid (5 vol%)	415 (24,200), 339 (14,800)	475	–[d]
	1,4-dioxane-acetic acid (20 vol%)	404 (24,700), 336 (15,500)	489	0.06
	1,4-dioxane-acetic acid (40 vol%)	389 (25,400), 314 (13,200)	498	0.17
	acetic acid	384 (24,000), 312 (10,000)	509	0.2

[a] 2.5×10^{-5} M.
[b] 2.5×10^{-6} M.
[c] The Φ values were determined by using a calibrated integrating sphere system ($\lambda_{ex} = 325$ nm).
[d] Too weak (Φ << 0.01).

a low fluorescence intensity (Φ = 0.03–0.04). The absorption bands of **1c**–**1e** appeared at around 385 nm, which was blue-shifted by *ca.* 30 nm, and the absorption band at around 350 nm became broader compared with that observed in 1,4-dioxane. The corresponding fluorescence maxima were observed at around 500–520 nm, which were red-shifted by 10–30 nm compared with those in 1,4-dioxane. The absorption and fluorescence spectral data of **1a**–**1e** in solution are summarized in Table 1.

3.2. Fluorescence proton sensing properties of phenylaminonaphtho[1,2-d]oxazol-2-yl-type fluorophores

As described in the previous section, the compounds **1c**, **1d**, and **1e** exhibit a medium fluorescence quantum yield in acetic acid. Therefore, in order to investigate their possible use as a proton sensor, the absorption and fluorescence spectra of **1c**–**1e** were investigated in various concentrations of acidic solution, which were prepared by the addition of acetic acid to 1,4-dioxane (Table 2). In the fluorophores **1c**, **1d**, and **1e**, with the increase in the amount of acetic acid, the absorption band at around 410 nm was blue-shifted by 20 nm and the absorption band at around 340 nm became broad band. In the corresponding fluorescence spectra, the fluorescence band at around 490 nm was red-shifted with enhancement of the intensity. The Φ value is increased by at least 20-fold with the increase of acetic acid content from 0 vol% to 40 vol% in 1,4-dioxane, and the Φ value of 0.15–0.17 was reached. In contrast, with increasing concentration of acetic acid in 1,4-dioxane, the fluorescence intensities of **1a** and **1b** decreased dramatically and the fluorescent maxima underwent a red- shift, due to the increase in polarity of the solution. By way of example Fig. 2 shows the fluorescence spectra of **1a** and **1c** in various concentrations of acidic solution.

3.3. Fluorescence enhancement behavior with an increase of water content in organic solvents

Of particular interest are the photophysical properties of **1d** in a mixture of an organic solvent and water. As shown in Fig. 3, the absorption and fluorescence spectra undergo only small changes on

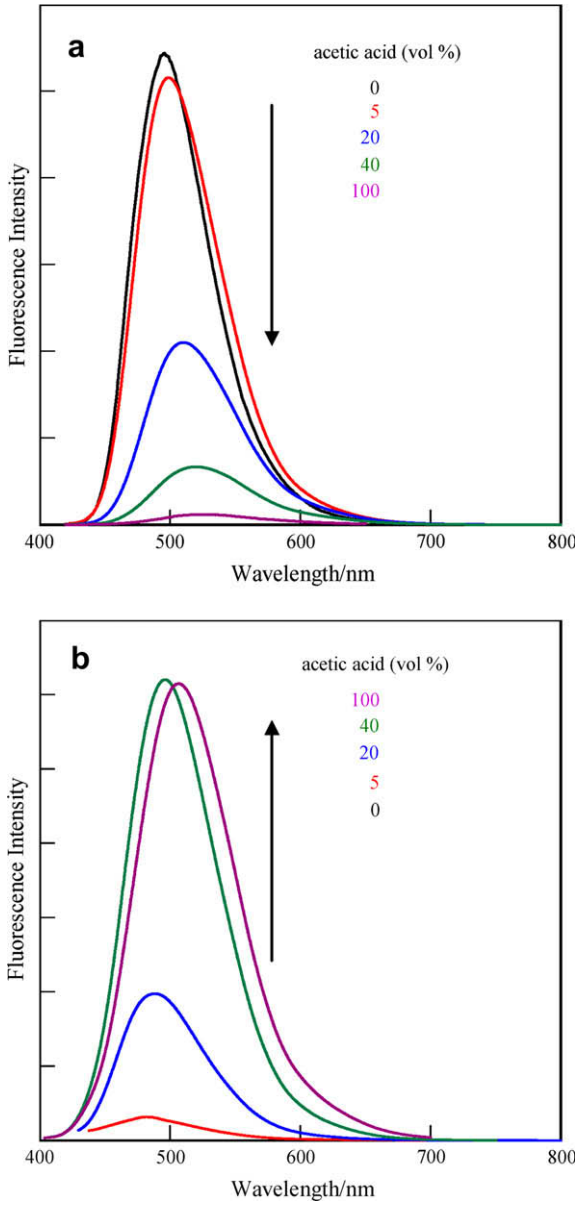

Fig. 2. Fluorescence spectra of (a) **1a** and (b) **1c** in acetic acid/1,4-dioxane mixture with different volume fractions of acetic acid ([1a] = [1c] = 2.5×10^{-5} M), respectively.

changing from 1,4-dioxane to 1,4-dioxane containing 15 vol% water. Upon the increasing of water content from 30 vol% to 45 vol%, the absorption and fluorescence spectra exhibit significant changes: the absorption band at around 410 nm was blue-shifted by 20 nm and the absorption band at around 340 nm became broad band, together with isosbestic point at 395 nm. In the corresponding fluorescence spectra, the fluorescence band at around 490 nm was slightly blue-shifted with enhancement of the intensity. In 1,4-dioxane containing 45 vol% water, the fluorescence quantum yield of 0.18 was achieved (Table 3). In acetone or ethanol containing 45 vol% water, the similar absorption and fluorescence spectral changes were observed. However, such absorption and fluorescence properties were not observed in the cases of **1a**, **1b**, **1c**, and **1e**. With increasing concentration of water in 1,4-dioxane, the fluorescence intensities of **1a** and **1b** decreased dramatically and the fluorescent maxima underwent a red- shift, due to the increase in polarity of the solution. In contrast, there are the fluorescent dyes such as 1,8-naphthalimide derivatives, whose fluorescence quantum yield in water is higher than that in organic solvents

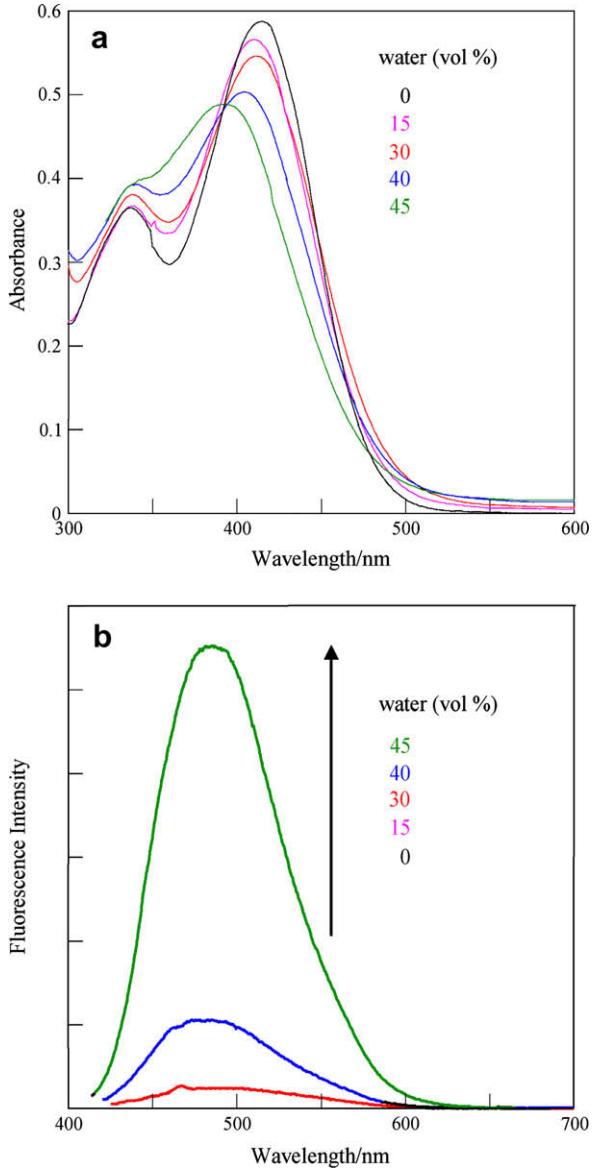

Fig. 3. (a) Absorption and (b) fluorescence spectra of **1d** in water/1,4-dioxane mixture with different volume fractions of water ([**1d**] = 2.5×10^{-5} M), respectively.

because of a change in the microscopic polarity around the fluorophore [43,44]. Although the compounds **1c**–**1e** belong to the same category because the all of them have a diethylamino group as a proton acceptor and similar dipole moments, only **1d** with a carboxyl group as a proton donor exhibits the enhancements in the fluorescence intensity with increasing concentrations of water in 1,4-dioxane. Therefore, the enhancement of fluorescence intensity of **1d** would not be attributable to a change in the microscopic polarity around the fluorophore with increasing concentrations of water in 1,4-dioxane. In fact, a clear isosbestic point and blue-shift of absorption maximum with increasing concentrations of water in 1,4-dioxane in the absorption spectra suggest the formation of a second species and a third species with two equilibria.

3.4. Semi-empirical MO calculations (AM1, CNDO/S)

To understand the photophysical properties of phenylaminonaphtho[1,2-*d*]oxazol-2-yl-type fluorophores, we have carried out semi-empirical molecular orbital (MO) calculations of **1a**–**1e** by the CNDO/S method [37–40] after geometrical optimizations MOPAC/AM1 method [36]. The calculated absorption wavelengths and the nature of the transition of the first absorption bands are collected in Table 4. As shown in Fig. 4, the optimized geometries of **1a**–**1e** show that the torsion angles between the naphthoxazole ring and the *p*-cyanophenyl or the p-carboxyphenyl group are 0.20°–8.80° for the all compounds. This result shows that the two rings are essentially coplanar to each other. On the other hand, the *p*-diethylaminophenyl or the p-butylphenyl groups are twisted from the plane of the naphthoxazole ring by about 50° for all the compounds.

Table 3
Spectroscopic properties of **1a**–**1e** in solvent-water

	Solvent	λ_{max}^{abs}/nm[a] [ε_{max}/dm^3 mol^{-1} cm^{-1}]	λ_{max}^{fl}/nm[b]	Φ[c]
1a	1,4-dioxane (water free)	407 (24,200), 335 (8700)	495	0.92
	1,4-dioxane-water (45 vol%)	414 (21,900), 334 (8300)	548	0.02
1b	1,4-dioxane (water free)	400 (20,700), 336 (8600)	491	0.95
	1,4-dioxane-water (45 vol%)	396 (22,700), 335 (10,800)	508	0.04
1c	1,4-dioxane (water free)	420 (25,300), 350 (15,500)	483	–[d]
	1,4-dioxane-water (45 vol%)	426 (21,200), 340 (14,000)	534	0.02
1d	1,4-dioxane (water free)	413 (23,800), 338 (15,400)	490	–[d]
	1,4-dioxane-water (15 vol%)	413 (23,300), 338 (15,400)	490	–[d]
	1,4-dioxane-water (30 vol%)	411 (21,900), 338 (15,600)	490	0.02
	1,4-dioxane-water (40 vol%)	404 (20,100), 338 (15,800)	487	0.03
	1,4-dioxane-water (45 vol%)	392 (19,800), 338 (15,900)	486	0.18
	acetone (water free)	413 (21,100), 338 (13,600)	508	–[d]
	acetone-water (45 vol%)	396 (–)[e], 337 (13,400)	495	0.08
	ethanol (water free)	400 (20,700), 328 (13,400)	493	–[d]
	ethanol-water (45 vol%)	390 (–)[e], 325 (–)[e]	495	0.17
1e	1,4-dioxane (water free)	415 (25,800), 337 (15,800)	500	–[d]
	1,4-dioxane-water (45 vol%)	419 (–)[e] , 338 (–)[e]	541	–[d]

[a] 2.5×10^{-5} M.
[b] 2.5×10^{-6} M.
[c] The Φ values were determined by using a calibrated integrating sphere system (λ_{ex} = 325 nm).
[d] Too weak (Φ << 0.01).
[e] Poor solubility.

The calculated absorption wavelengths and the oscillator strength values are comparable with the observed spectra in 1,4-dioxane, although the calculated absorption spectra are blue-shifted. This deviation of the CNDO/S calculations, giving high transition energies compared with the experimental values, has been generally observed [45]. The calculations show that the longest excitation bands for **1a**–**1e** are mainly assigned to the transition from the HOMO to the LUMO, where HOMO is mostly localized on the aminonaphtho[1,2-*d*]oxazol moiety, and the LUMO is mostly localized on the *p*-cyanophenyl or the *p*-carboxyphenyl moiety. The changes in the calculated electron density accompanying the first electron excitation are shown in Fig. 4, which show a strong migration of intramolecular charge-transfer character from the aminonaphtho[1,2-*d*]oxazol moiety to the *p*- cyanophenyl or the *p*-carboxyphenyl moiety in all the dyes. It is noteworthy that the *p*-butylphenyl moiety of **1a** and **1b** and the *p*-diethylaminophenyl moiety of **1c**–**1e** barely participate in the intramolecular charge-transfer. For the all compounds, the values of the dipole moments in the ground states are 4.17–8.69 D and the differences between the dipole moments ($\Delta\mu$) of the first excited and the ground states are 10.06–13.14 D. These calculations indicate that the compounds **1a**–**1e** have large dipole moments in the excited state, which explains well the experimental observations that the compounds show a bathochromic shift of their fluorescence maxima in polar solvents and the Stokes shift values for the compounds in polar solvents are much larger than those in non-polar solvents.

Furthermore, we estimated the photophysical properties for **1c**–**1e** with the protonated diethylamino group, because it was assumed that the diethylamino nitrogen is protonated in acidic solution. The calculated absorption wavelengths of **1cH$^+$**–**1eH$^+$**

Table 4
Calculated absorption spectra for **1a**–**1e**, **1cH**$^+$–**1eH**$^+$ with the protonated diethylamino group, **1d** (anion form) with the deprotonated carboxyl group, and **1d** with zwitter-ion form

Quinol	μ/D[a]	Absorption (calc.)		CI component[c]	$\Delta\mu$/D[d]
		λ_{max}/nm	f[b]		
1a	5.61	410	0.86	HOMO → LUMO (90%)	11.46
1b	8.69	414	0.83	HOMO → LUMO (88%)	12.42
1c	4.17	409	0.87	HOMO → LUMO (90%)	11.31
1d	7.64	420	0.85	HOMO → LUMO (88%)	13.14
1e	6.65	400	0.79	HOMO → LUMO (91%)	10.06
1cH$^+$	29.35	385	0.93	HOMO → LUMO (83%)	6.13
1dH$^+$	32.86	384	0.87	HOMO → LUMO (87%)	7.23
1d (anion form)	37.10	378	0.92	HOMO → LUMO (91%)	0.93
1d (zwitter-ion form)	61.17	405	0.50	HOMO-1 → LUMO (66%)	15.97
1eH$^+$	35.10	378	0.84	HOMO → LUMO (64%)	4.87

[a] The values of the dipole moment in the ground state.
[b] Oscillator strength.
[c] The transition is shown by an arrow from one orbital to another, followed by its percentage CI (configuration interaction) component.
[d] The values of the difference in the dipole moment between the excited and the ground states.

with the protonated diethylamino group are shifted to shorter wavelengths compared to those of the neutral **1c**–**1e**, which is in good agreement with the experimental data in acidic solution. The calculations also show that the longest excitation bands for **1cH**$^+$–**1eH**$^+$ are mainly assigned to the transition from the HOMO to the LUMO, where the HOMO is mostly localized on the aminonaphtho[1,2-*d*]oxazol moiety, and the LUMO is localized on the protonated *p*-diethylaminophenyl and the *p*-cyanophenyl or the *p*-carboxyphenyl moieties. The changes in the calculated electron density accompanying the first electron excitation are shown in Fig. 4, which shows a strong migration of the intramolecular charge-transfer character form the aminonaphtho[1,2-*d*]oxazol moiety to the protonated *p*-diethylaminophenyl and the *p*-cyanophenyl or the *p*-carboxyphenyl moieties. The values of the dipole moments in the ground states of **1cH**$^+$–**1eH**$^+$ (29.35–35.10 D) are significantly large compared to those of the neutral **1c**–**1e**.

3.5. Mechanism of the fluorescence enhancement behavior with increase of water or acid contents in organic solvents

On the bases of the calculations and the spectral analyses, we considered that the absorption and fluorescence properties of **1d** in a mixture of an organic solvent and water was associated with the protonation of the diethylamino group by the intramolecular proton transfer from the carboxyl group via deprotonation of the carboxyl group, because a addition of water in organic solvents promoted the dissociation of the carboxyl proton of **1d**. From the Fig. 3, the clear isosbestic point and blue-shift of absorption maximum with increasing concentrations of water in 1,4-dioxane in absorption spectra suggests that three distinct species are present in two equilibria. Thus, at first, a blue-shift of absorption maximum with increasing concentrations of water in 1,4-dioxane would be attributed to the deprotonation of the carboxyl group of **1d**, so that the deprotonated **1d** is formed at the first equilibrium (Fig. 5b; anion form **1d**′). Such a blue-shift of absorption spectra has also been observed for other organic dyes with carboxyl group in polar or alcohol solution [5,46–48]. Furthermore, upon increasing the water content, the diethylamino group was protonated via the deprotonation of the carboxyl group; the zwitter-ion structure is formed at the second equilibrium (Fig. 5b; zwitter-ion form **1d**″). Consequently, it was concluded that the fluorescent dye **1d** is an example of photo-induced electron transfer (PET) [1–5,7–22], which in this case takes place from the diethylamino group to the naphtho[1,2-*d*]oxazole fluorophore skeleton, and cannot exhibit fluorescent emission. When the diethylamino group was protonated via the deprotonation of the carboxyl group, the electron transfer is prevented, the structure became the fluorescent zwitter-ion form, and a drastic fluorescence enhancement was observed (Fig. 5a,b). In fact, the MO calculations revealed that the calculated absorption wavelengths of the anion and zwitter-ion forms of **1d** are slightly shifted to shorter wavelengths compared to that of the neutral **1d** (Table 3), which is in good agreement with the experimental data in a mixture solvent of organic solvent and water (Table 4). Thus, the fluorophores **1a** without both the carboxyl and

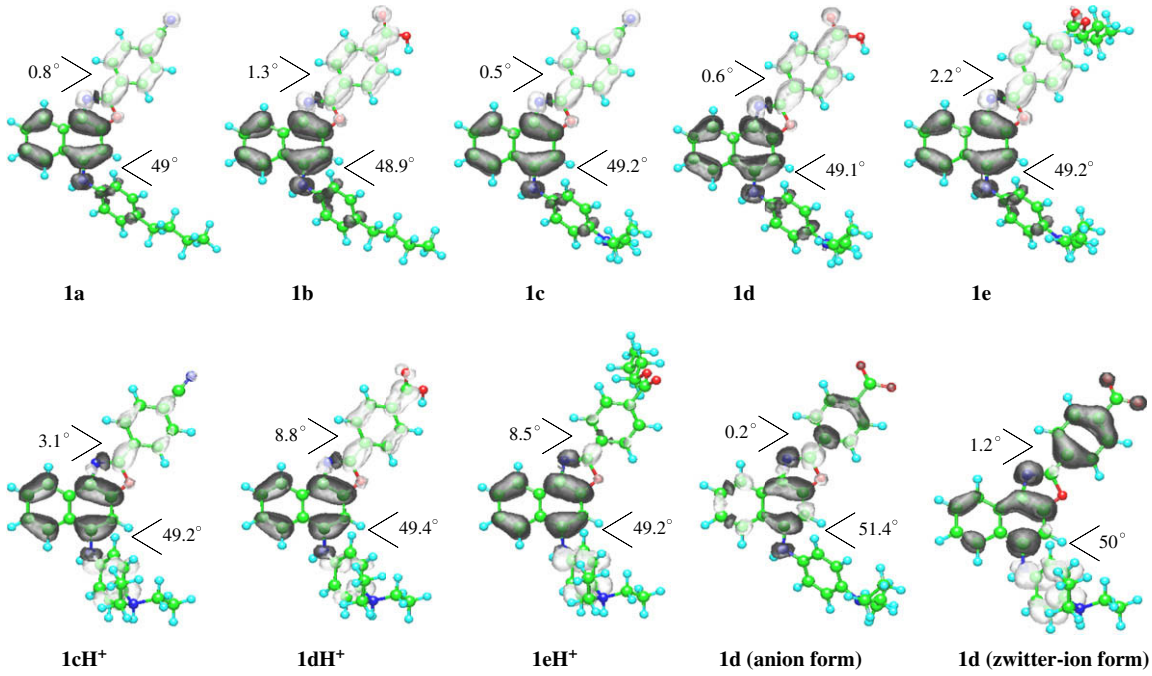

Fig. 4. Calculated electron density changes accompanying the first electronic excitation of **1a**–**1e**, **1cH**$^+$–**1eH**$^+$ with the protonated diethylamino group, **1d** (anion form) with the deprotonated carboxyl group, and **1d** with zwitter-ion form. The black and white lobes signify degreases and increase in electron density accompanying the electronic transition. Their areas indicate the magnitude of the electron density change.

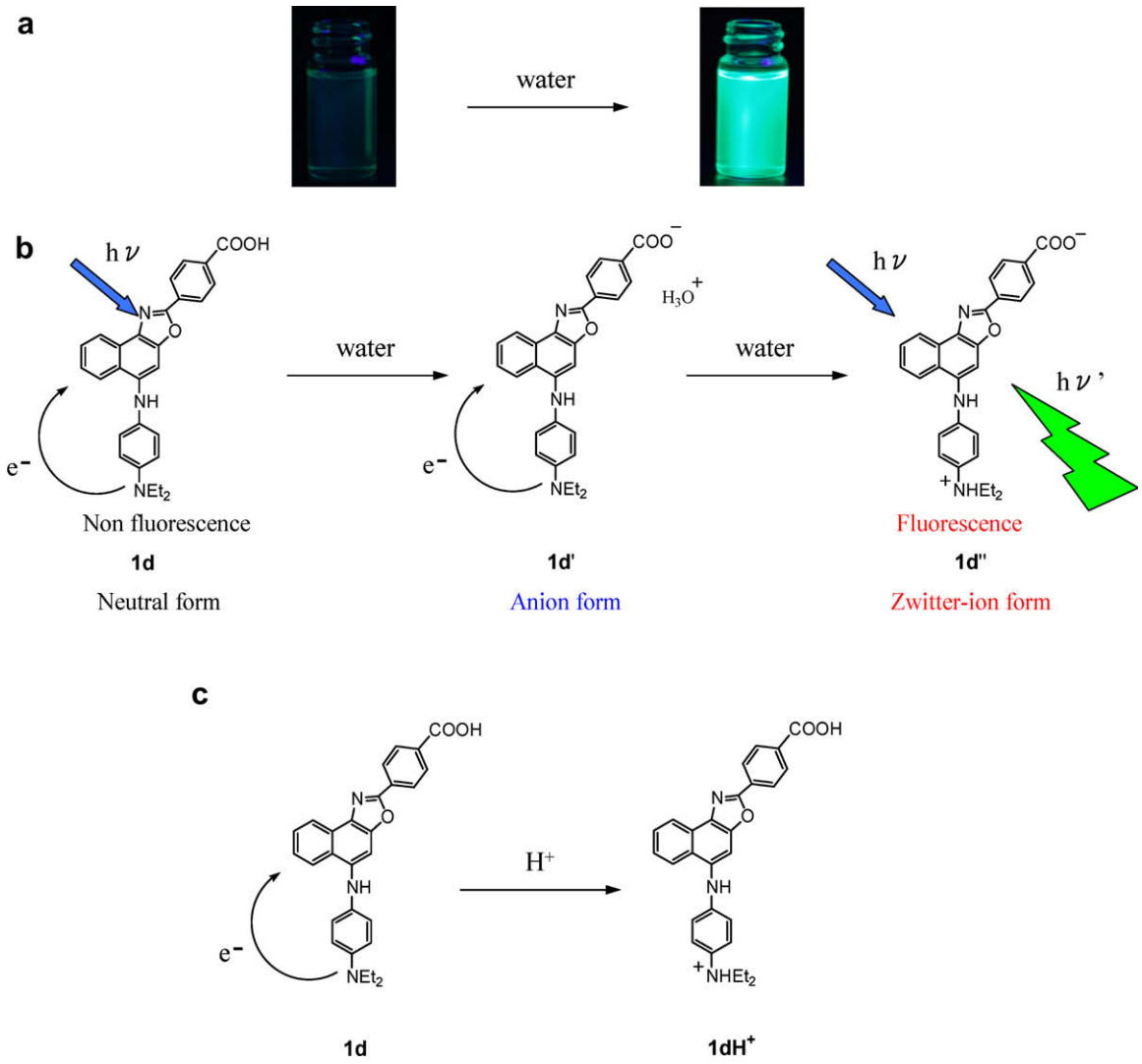

Fig. 5. (a) Photograph of **1d** before and after addition of water to 1,4-dioxane solution under irradiation at 365 nm, (b) proposed mechanism for fluorescent water-sensor **1d** by PET, and (c) mechanism of fluorescent proton-sensor **1d** by PET.

diethylamino groups, **1b** without the diethylamino group, and **1c** and **1e** without the carboxyl group cannot function as a fluorescent dye for sensing water by PET. Moreover, **1d** sodium salt (–COONa) which was prepared by the treatment of **1d** by sodium hydroxide solution, does not exhibit a fluorescent enhancement upon the increasing of water content in solution, this result also demonstrates that a drastic fluorescent enhancement of **1d** having carboxyl group (–COOH) upon the increasing of water content in solution is attributable to suppression of PET by the intramolecular proton transfer of the carboxyl proton to diethylamino group. On the other hand, the fluorescence properties of **1c**–**1e** in acetic acid are assumed to be caused by protonation of the diethylamino group by intermolecular proton transfer from the acetic acid (Fig. 5c).

4. Conclusions

A new class of fluorescent dyes for sensing proton and water in organic solvents based on phenylaminonaphtho[1,2-*d*]oxazol-2-yl-type fluorophore with the proton donor and acceptor sites have been designed and developed, and their photophysical properties were investigated in various solution. The fluorophore with both the carboxyl and diethylamino groups exhibits a feeble fluorescent property in organic solvents because of PET, which takes place from the diethylamino group to the naphtho[1,2-*d*]oxazole fluorophore skeleton. With increasing concentrations of water in organic solvents, a dramatic fluorescence enhancement is observed, which is attributable to suppression of PET by the intramolecular proton transfer of the carboxyl proton to the diethylamino group: when the diethylamino group was protonated, the electron transfer is prevented, the structure became the fluorescent zwitter-ion form. Thus, a new concept for the molecular design of a fluorescent dye for sensing water in organic solvents by PET has been demonstrated. In addition, it was demonstrated that the phenylaminonaphtho[1,2-*d*]oxazol-2-yl-type fluorophores are of considerable promise for use as novel proton sensor.

Acknowledgments

This work was partially supported by a Grant-in-Aid for Science and Research from the Ministry of Education, Science, Sport and Culture of Japan (Grant 18350100) and by a Special Research Grant for Green Science from Kochi University.

References

[1] Lakowicz JR, Thompson RB. Advances in fluorescence sensing technology. Rellingham WA: V: SPIE; 2001.

[2] Gzarnik AW. Fluorescent chemosensors for ion and molecule recognition. In: ACS Symposium Series No. 538. Washington DC: American Chemical Society; 1992.
[3] Gzarnik AW. Chemical communication in water using fluorescent chemosensors. Acc Chem Res 1994;27(10):302–8.
[4] de Silva AP, Gunaratne HQN, Gunnlaugsson T, Huxley AJM, McCoy CP, Rademacher JT, et al. Signaling recognition events with fluorescent sensors and switches. Chem Rev 1997;97(5):1515–66.
[5] Valeur B. Molecular fluorescence. Weinheim: WILEY-VCH; 2002.
[6] Balzani V, Venturi M, Credi A. Molecular devices and machines. Weinheim: WILEY-VCH; 2003.
[7] Aoki I, Sakaki T, Shinkai S. A new metal sensory system based on intramolecular fluorescence quenching on the ionophoric calix[4]arene ring. J Chem Soc Chem Commun 1992;9:730–2.
[8] de Silva AP, Gunaratne HQN, Maguire GEM. 'Off-on' fluorescent sensors for physiological levels of magnesium ions based on photoinduced electron transfer (PET), which also behave as photoionic OR logic gates. J Chem Soc Chem Commun 1994;10:1213–4.
[9] Parker D, Williams JAG. Luminescence behaviour of cadmium, lead, zinc, copper, nickel and lanthanide complexes of octadentate macrocyclic ligands bearing naphthyl chromophores. J Chem Soc Perkin 1995;2:1305–14.
[10] de Silva AP, Stewart S. Switching 'on' the luminescence of one metal ion with another: selectivity characteristics with respect to the emitting and triggering metal. J Chem Soc Chem Commun 1997;19:1891–2.
[11] Kubo K, Kato N, Sakurai T. Synthesis and complexation behavior of diaza-18-crown-6 carrying two pyrenylmethyl groups. Bull Chem Soc Jpn 1997;70(12):3041–6.
[12] Unob F, Asfari Z, Vicens J. An anthracene-based fluorescent sensor for transition metal ions derived from calix[4]arene. Tetrahedron Lett 1998;39(19):2951–4.
[13] Hirano T, Kikuchi K, Urano Y, Higuchi T, Nagano T. Novel zinc fluorescent probes excitable with visible light for biological applications. Ang Chim Int Ed 2000;39(6):1052–4.
[14] Walkup GK, Burdette SC, Lippard SJ, Tsien RY. A new cell-permeable fluorescent probe for Zn^{2+}. J Am Chem Soc 2000;122(23):5644–5.
[15] de Silva AP, de Silva SA. Fluorescent signalling crown ethers; 'switching on' of fluorescence by alkali metal ion recognition and binding in situ. J Chem Soc Chem Commun 1986;23:1709–10.
[16] Huston ME, Haider KW, Czarnik AW. Chelation enhanced fluorescence in 9,10-bis[[(2-(dimethylamino)ethyl)methylamino]methyl]anthracene. J Am Chem Soc 1988;110(13):4460–2.
[17] Fages F, Desvergne JP, Bouas-Laurent H, Marsau P, Lehn JM, Kotzyba-Hibert F, et al. Anthraceno-cryptands: a new class of cation-complexing macrobicyclic fluorophores. J Am Chem Soc 1989;111(23):8672–80.
[18] Akkaya EU, Huston ME, Czarnik AW. Chelation-enhanced fluorescence of anthrylazamacrocycle conjugate probes in aqueous solution. J Am Chem Soc 1990;112(9):3590–3.
[19] de Silva AP, Gunaratne HQN, Sandanayake KRAS. A new benzo-annelated cryptand and a derivative with alkali cation-sensitive fluorescence. Tetrahedron Lett 1990;31(36):5193–6.
[20] Fabbrizzi L, Licchelli M, Pallavicini P, Perotti A, Sacchi D. An anthracene-based fluorescent sensor for transition metal ions. Ang Chim Int Ed 1994;33(19):1975–7.
[21] Fabbrizzi L, Licchelli M, Pallavicini P, Taglietti A. A zinc(II)-driven intramolecular photoinduced electron transfer. Inorg Chem 1996;35(6):1733–6.
[22] de Santis G, Fabbrizzi L, Licchelli M, Mangano C, Sacchi D, Sardone N. A fluorescent chemosensor for the copper(II) ion. Inorg Chim Acta 1997;257(1):69–76.
[23] Kessler MA, Gailer JG, Wolfbeis OS. Optical sensor for on-line determination of solvent mixtures based on a fluorescent solvent polarity probe. Sens Actuators B 1991;3(4):267–72.
[24] Bai M, Seiz WR. A fiber optic sensor for water in organic solvents based on polymer swelling. Talanta 1994;41(6):993–9.
[25] Liu W, Wang Y, Jin W, Shen G, Yu R. Solvatochromogenic flavone dyes for the detection of water in acetone. Anal Chim Acta 1999;383(3):299–303.
[26] Mishra H, Misra V, Mehata MS, Pant TC, Tripathi HB. Fluorescence studies of salicylic acid doped poly(vinyl alcohol) film as a water/humidity sensor. J Phys Chem A 2004;108(12):2346–52.
[27] Chang Q, Murtaza Z, Lakowicz JR, Rao G. A fluorescence lifetime-based solid sensor for water. Anal Chim Acta 1997;350(1):97–104.
[28] Glenn SJ, Gullum BM, Nair RB, Nivens DA, Murphy CJ, Angel SM. Lifetime-based fiber-optic water sensor using a luminescent complex in a lithium-treated Nafion™ membrane. Anal Chim Acta 2001;448(1):1–8.
[29] Yang X, Niu CG, Shang ZJ, Shen GL, Yu RQ. Optical-fiber sensor for determining water content in organic solvents. Sens Actuators B 2001;75(1):43–7.
[30] Citterio D, Minamihashi K, Kuniyoshi Y, Hisamoto H, Sasaki S, Suzuki K. Optical determination of low-level water concentrations in organic solvents using fluorescent acridinyl dyes and dye-immobilized polymer membranes. Anal Chem 2001;73(21):5339–45.
[31] Niu CG, Guan AL, Zeng GM, Liu YG, Li ZW. Fluorescence water sensor based on covalent immobilization of chalcone derivative. Anal Chim Acta 2006;577(2):264–70.
[32] Niu CG, Qin PZ, Zeng GM, Gui XQ, Guan AL. Fluorescence sensor for water in organic solvents prepared from covalent immobilization of 4-morpholinyl-1,8-naphthalimide. Anal Bioanal Chem 2007;387(3):1067–74.
[33] Orellana G, Gomez-Carneros AM, de Dios C, Garcia-Martinez AA, Moreno-Bondi MC. Reversible fiber-optic fluorosensing of lower alcohols. Anal Chem 1995;67(13):2231–8.
[34] Choi MMF, Tse OL. Humidity-sensitive optode membrane based on a fluorescent dye immobilized in gelatin film. Anal Chim Acta 1999;378(1):127–34.
[35] Ooyama Y, Egawa H, Yoshida K. A new class of fluorescent dye for sensing water in organic solvents by photo-induced electron transfer: phenylaminonaphtho[1,2-d]oxazol-2-yl-type fluorophore with both proton binding and proton donating sites. Eur J Org Chem DOI: 10.1002/ejoc.200800606.
[36] Dewar MJS, Zoebisch EG, Healy EF, Stewart JJP. Development and use of quantum mechanical molecular models. 76. AM1: a new general purpose quantum mechanical molecular model. J Am Chem Soc 1985;107(13):3902–9.
[37] Ridley JE, Zerner MC. An intermediate neglect of differential overlap technique for spectroscopy: pyrrole and the azines. Theor Chim Acta 1973;32(2):111–34.
[38] Ridley JE, Zerner MC. Triplet states via intermediate neglect of differential overlap: benzene, pyridine and the diazines. Theor Chim Acta 1976;42(3):223–36.
[39] Bacon AD, Zerner MC. An intermediate neglect of differential overlap theory for transition metal complexes: Fe, Co and Cu chlorides. Theor Chim Acta 1979;53(1):21–54.
[40] Kurtz HA, Stewart JJP, Dieter KM. Calculation of the nonlinear optical properties of molecules. J Comput Chem 1990;11(1):82–7.
[41] Würthner F, Ahmed S, Thalacker C, Debaerdemaeker T. Core-substituted naphthalene bisimides: new fluorophors with tunable emission wavelength for FRET studies. Chem Eur J 2002;8(20):4742–50.
[42] Shen Z, Röhr H, Rurack K, Uno H, Spieles M, Schuls B, et al. Boron-diindomethene (BDI) dyes and their tetrahydrobicyclo precursors – en route to a new class of highly emissive fluorophores for the red spectral range. Chem Eur J 2004;10(19):4853–71.
[43] Ramachandram B, Sankaran NN, Karmarkar R, Saha S, Samanta A. Fluorescence signalling of transition metal ions by multi-component systems comprising 4-chloro-1,8-naphthalimide as fluorophore. Tetrahedron 2000;56(36):7041–4.
[44] Ramachandram B, Saroja G, Sankaran NB, Samanta A. Unusually high fluorescence enhancement of some 1,8-naphthalimide derivatives induced by transition metal salts. J Phys Chem B 2000;104(49):11824–32.
[45] Adachi M, Nakamura S. Comparison of the INDO/S and the CNDO/S method for the absorption wavelength calculation of organic dyes. Dyes Pigm 1991;17(4):287–96.
[46] Hagberg DP, Edvinsson T, Marinado T, Boschloo G, Hagfeldt A, Sun L. A novel organic chromophore for dye-sensitized nanostructured solar cells. Chem Commun 2006:2245–7.
[47] Qin P, Yang X, Chen R, Sun L, Marinado T, Edvinsson T, et al. Influence of π-conjugation units in organic dyes for dye-sensitized solar cells. J Phys Chem C 2007;111(4):1853–60.
[48] Yen YS, Hsu YC, Lin JT, Chang CW, Hsu CP, Yin DJ. Pyrrole-based organic dyes for dye-sensitized solar cells. J Phys Chem C 2007;112(32):12557–67.